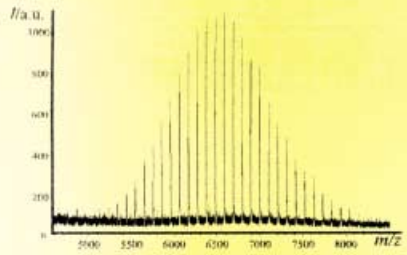

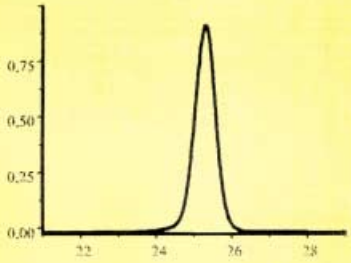

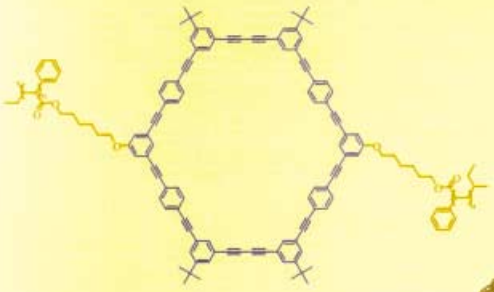

Coil-Ring-Coil Block Copolymers: Synthesis and Solid-State Structure

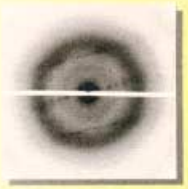

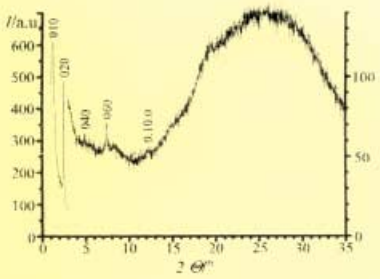

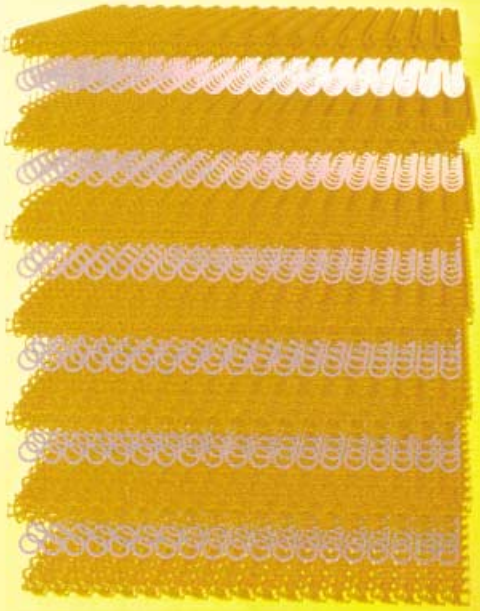

For more information see the following pages.

 DOI: 10.1002/chem.200304796

Synthesis and Solid-State Organization of Coil – Ring – Coil Block Copolymers

Silvia Rosselli,[a] Anne-Désirée Ramminger,[a] Thomas Wagner,[a] Günter Lieser,*[a] and Sigurd Höger*[a,b]

Dedicated to Professor Manfred T. Reetz on the occasion of his 60th birthday

Abstract: Shape-persistent macrocycles based on the phenyl-ethynyl-butadienyl backbone containing two extraannular hydroxyl groups were prepared by the oxidative coupling of the appropriate phenylethynyl oligomers. Carbodiimide-directed coupling with independently synthesized polystyrene carboxylic acid oligomers led to ABA coil – ring – coil block copolymers in which the central macrocycle serves as rigid and the polystyrene oligomers as flexible elements. Depending on the size of the coil blocks, these structures aggregate in cyclohexane into supramolecular hollow cylindrical brushes in which the rigid core is surrounded by the flexible matrix. However, in the solid state it is not possible to identify a morphology in which isolated channels based on aggregated macrocycles are embedded in a matrix of polystyrene. Detailed X-ray and electron diffraction studies on samples prepared from a solution in cyclohexane under equilibrium conditions show that the material adopts a lamellar morphology in the solid state in which columns of macrocycles are aggregated into layers which are separated by polystyrene.

Keywords: macrocycles · nanostructures · polymers · supramolecular chemistry

Introduction

The understanding of the design principles for molecular building blocks that can self-assemble into well-defined structures is the basis for the construction of aggregates with a high degree of complexity. In the field of polymer science, the synthesis, investigation, and theoretical description of block copolymers composed of two or more flexible blocks that phase separate into a variety of morphologies has made significant progress over the last decades. It is the basis for many materials used today.

During the last decade, the aggregation behavior of block copolymers in which at least one block is more or less rigid and another is rather flexible (rod – coil block copolymers) has attracted increasing attention. This provides an opportunity for the formation of supramolecular nanostructures arising from the microphase separation of the rod and the coil blocks.[1] The aggregation of the rigid segments into liquid-crystalline domains that is observed even at relatively low degrees of polymerization is a result of the high incompatibility of the different blocks. The kind of nanostructure that is actually formed depends on the nature of the blocks, the total molecular weight of the polymer and the volume fraction of the rigid and the flexible blocks, respectively.[2]

Recently, we described a new class of rod – coil block copolymers in which the rigid segment is a nanometer-sized shape-persistent macrocycle to which two polystyrene (PS) blocks are covalently attached leading to coil – ring – coil block copolymers (Figure 1).[3, 4]

Figure 1. Schematic presentation of coil – ring – coil block copolymers.

Due to its structure, the rigid part of the molecule can no longer be described as one-imensional but has a similar expansion in the second dimension. In contrast to disklike molecules, these noncollapsed macrocycles have a nanoscale hollow interior that allows the arrangement of functional

[a] Prof. Dr. S. Höger, Dr. G. Lieser, Dr. S. Rosselli, A.-D. Ramminger, T. Wagner
Max Planck Institute for Polymer Research
Ackermannweg 10, 55128 Mainz (Germany)
Fax: (+49) 6131-379-100
E-mail: lieser@mpip-mainz.mpg.de

[b] Prof. Dr. S. Höger,
New address: Universität Karlsruhe
Polymer-Institut, Hertzstrasse 16, 76187 Karlsruhe (Germany)
Fax: (+49) 721-608-4421
E-mail: hoeger@chemie.uni-karlsruhe.de.

DOI: 10.1002/chem.200304796

groups in a convergent way.[5, 6] In addition, a columnar arrangement of the macrocycles could lead to the formation of supramolecular (intraannular functionalized) channel structures.[7]

Owing to the attachment of the flexible side groups, the solubility of the otherwise only moderately soluble rigid block is largely enhanced. As reported previously, some of the coil – ring – coil triblock copolymers **1** are even soluble in the non-polar solvent cyclohexane, a Θ-solvent for polystyrene but not for the rigid core.[8] Of course, the solubilizing influence of the polystyrene block increases with increasing molecular weight.[9]

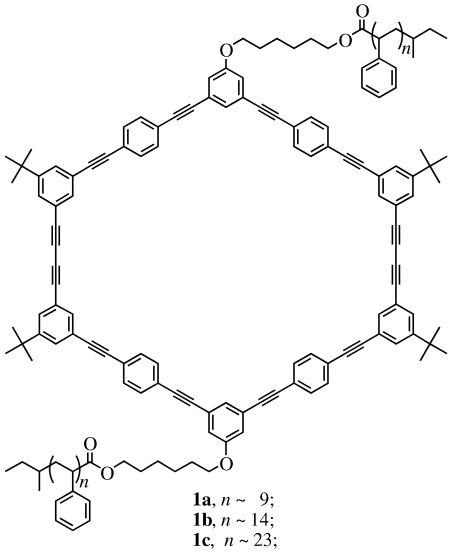

1a, $n \sim 9$;
1b, $n \sim 14$;
1c, $n \sim 23$;
1d, $n \sim 32$;
1e, $n \sim 50$;

While **1e** is easily soluble in cyclohexane and the solution shows no unusual viscosity or birefringence, **1a** in warm cyclohexane forms only a suspension. Of special interest is **1c** (M_w of each PS block $\sim 500\,g\,mol^{-1}$) which dissolves well in warm cyclohexane and upon cooling to room temperature rapidly forms a very viscous solution. At the same time the solution becomes strongly birefringent. These observations were the starting point for a more detailed investigation into solutions of **1c** in cyclohexane. Scattering experiments in solution as well as investigations on solid samples prepared under "nonequilibrium conditions" (i.e. by fast solvent evaporation) revealed that the block copolymer aggregates in solution into supramolecular hollow cylinderical brushes with an external diameter of about 10 nm and a lumen of about 2 nm. It can be assumed that in solution the rigid core of the brushes is isotropically surrounded by the flexible PS corona (Figure 2).

However, the solid-state structure of samples of these block copolymers prepared under "equilibrium conditions" (i.e. by slow solvent evaporation) has not yet been investigated. With reference to "hairy rod molecules", in which the central rod is bound covalently, models of the aggregation behavior could either be tubes of aggregated macrocycles formed by the supramolecular cylindrical aggregates within a polystyrene matrix (model 1, Figure 3a), or layered structures of planar regular arrays of tubes interchanging with layers of amorphous polystyrene (model 2, Figure 3b).[10] Predictions as to which model better describes the aggregation behavior cannot be made easily.

Here we describe the synthesis of **1** and the detailed investigation of the solid-state structure of samples of **1c** prepared under equilibrium conditions.

Results and Discussion

Synthesis: Over the past several years we have prepared a variety of different shape-persistent macrocycles based on the phenyl-ethynyl-butadienyl backbone.[11] The cyclization reaction is the Cu^{I}/Cu^{II}-mediated Glaser coupling of rather rigid bisacetylenic precursors ("half-rings").[12] Their structure is designed in such a way that the coupling of only two bisacetylenes gives the shape-persistent cyclic structure. This is a compromise between the yield in the cyclization step and the effort required in the preparation of the precursor. Their preparation is routinely performed by a number of repetitive Hagihara coupling and silyl-deprotecting steps of appropriate monoprotected bisacetylenes. Synthesis of both the cyclization precursors and of the monoprotected bisacetylenes rely on the combination of side selectivity in the palladium catalyzed aryl – acetylene coupling and the different deprotection kinetics of silyl groups of different bulk. Aromatic bromoiodo compounds can first be selectively coupled with terminal acetylenes at the iodo position. Subsequent addition of a second acetylene will then lead to a coupling reaction at the bromo position.[13] Furthermore, both coupling reactions can be performed in a one-pot reaction to give unsymmetrically substituted bisacetylenes in high yields. Since bisacetylenes protected with trimethylsilyl (TMS) or triethylsilyl (TES) groups and triisopropylsilyl (TIPS) groups can be selectively deprotected at the TMS or TES position, respectively, monoprotected bisacetylenes are easily available from bromoiodo compounds (Scheme 1).[14]

Scheme 2 illustrates the synthesis of the half rings and their cyclization. Bromo-4-iodobenzene (**2**) was treated with TES-acetylene at room temperature overnight, and for an additional hour at 50 °C. Subsequently, a slight excess of 1-ethynyl-3-(2-triisopropylsilylethynyl)-5-*tert*-butylbenzene[11a] was add-

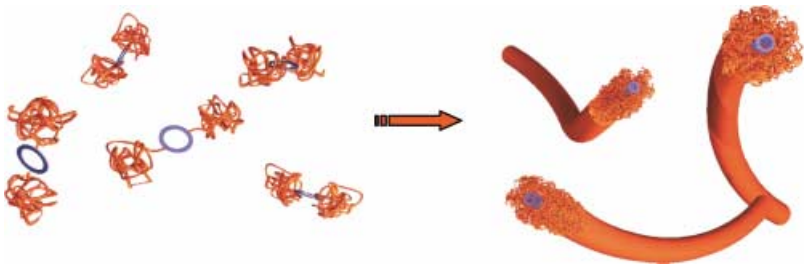

Figure 2. Aggregation of the coil – ring – coil block copolymers into hollow cylindrical brushes.

Figure 3. Possible aggregation of the cylindrical brushes in the solid state.

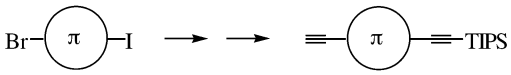

Scheme 1. Monoprotected bisacetylenes are prepared from the bromo-iodo compounds.

ed, and the mixture was stirred for an additional four days at the same temperature before workup. Deprotection of the TES group of **3** was performed by stirring with potassium carbonate in methanol/THF (1:1) for four days. Palladium-catalyzed coupling of **4** with the diiodide **5**, and desilylation of **6** by reaction with Bu_4NF gave **7**. $CuCl/CuCl_2$-promoted coupling of the half ring **7** was performed under pseudo-high-dilution conditions at 55 °C and gave the macrocycle **8** in 50 % yield after chromatography. The purity of the macrocycle was determined by NMR spectroscopy and mass spectrometry as well as by gel permeation chromatography (GPC), and showed the absence of trimers and higher oligomers. As we have explored previously, this elevated cyclization temperature is a compromise between the increased coupling rate favoring the dimer formation and the decreased product stability.[15] Base-catalyzed hydrolysis of the benzoate groups generated the macrocyclic diol **9**.

The synthesis of the polystyrene – carboxylic acid oligomer (PS-COOH) **10** was done by anionic polymerization of styrene in cyclohexane and subsequently adding the oligostyrene anion solution to a large excess of CO_2-saturated THF.[16] The oligomeric crude product could be purified

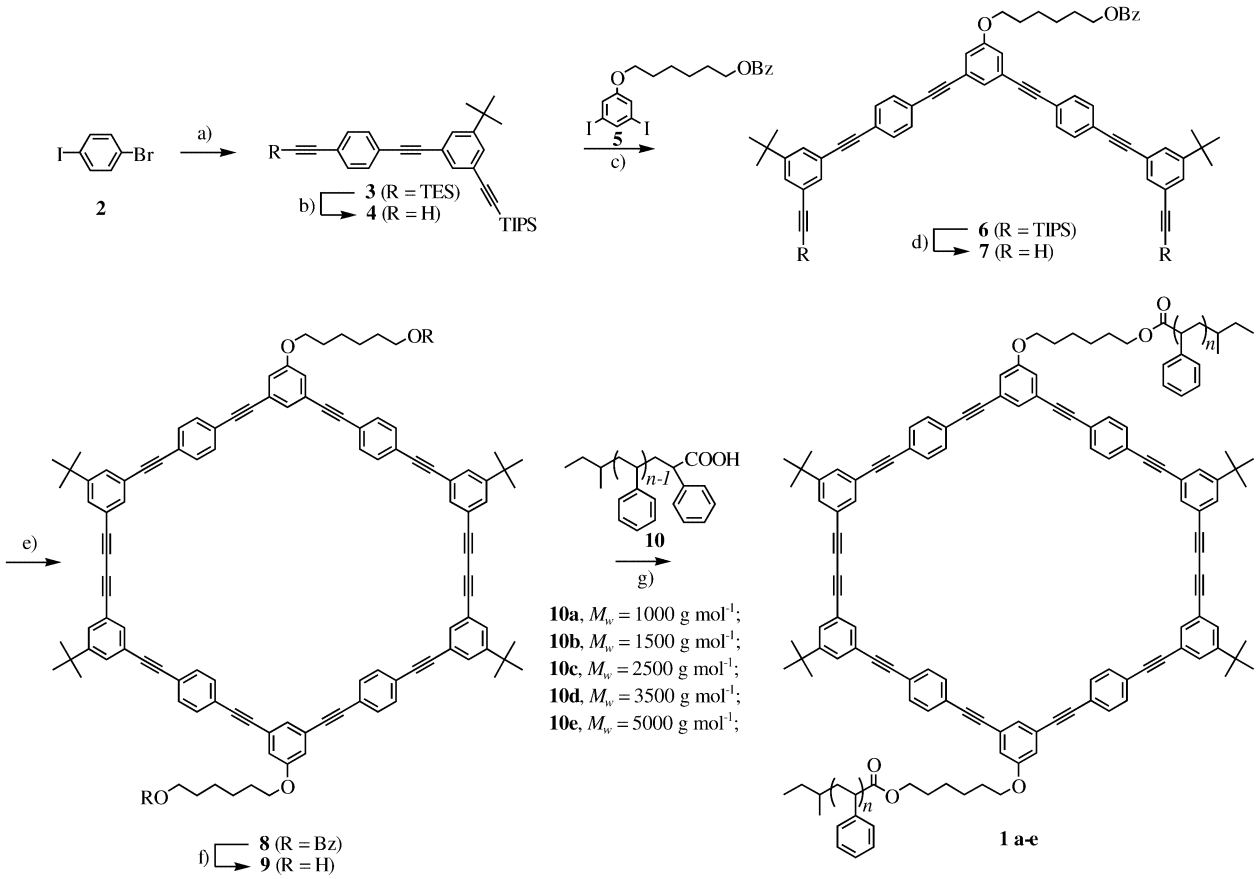

Scheme 2. a) 1. TES acetylene, Pd^0 (cat.), Cu^I (cat.), piperidine; 2. ethynyl-3-(2-triisopropylsilylethynyl)-5-*tert*-butylbenzene, 91 %; b) K_2CO_3, MeOH, THF, 83 %; c) Pd^0 (cat.), Cu^I (cat.), piperidine, 78 %; d) Bu_4NF, THF, 93 %; e) CuCl, $CuCl_2$, pyridine, 50 %; f) KOH; H_2O, THF, 87 %; g) DMAP/*p*-TsOH, diisopropyl carbodiimide, 32 – 86 %.

easily by column chromatography. Eluting with toluene removed all side products (mostly PS and di-PS ketone) and the PS-COOH was obtained by changing the eluent to THF.

Attachment of the PS-COOH to the macrocyclic diol was performed by the 4-dimethylaminopyridine (DMAP)/*p*-toluenesulfonic acid (*p*-TsOH)-catalyzed carbodiimide coupling overnight and purification of the crude reaction product by column chromatography.[17] The coupling could also be performed by esterification of **9** with the corresponding PS-carboxylic acid chloride or by reacting the macrocyclic diol with PS-COOH using diethylazodicarboxylate (DEAD)/PPh_3 (Mitsunobu conditions) as condensating reagents. However, in the first case the yield of the desired copolymer was very low (according to the GPC data, about 10 %) and we were not able to purify the material by column chromatography or precipitation. In the latter case the copolymer was formed in high yields but the material contained an impurity with double the molecular weight as observed by GPC. Again, pure ester **1** could not be obtained by simple column chromatography. Various amounts of a side product of similar molecular weight were also observed (GPC data) when an aqueous workup was carried out on the reaction mixture of the DMAP/*p*-TsOH-catalyzed carbodiimide coupling prior to the chromatographic purification. The nature and the origin of this side product could not be discovered. Nevertheless, changing the workup procedure solved this problem. After the carbodiimide coupling reaction was performed, the reaction solvent (CH_2Cl_2) was removed under reduced pressure and the solid residue chromatographed over silica gel. This operation turned out to be essential and gave the block copolymers **1** in reproducible purity.

All block copolymers **1** are readily soluble in chloroform, dichloromethane, THF, and toluene and were characterized by NMR spectroscopy, GPC, and matrix-assisted laser desorption ionization time-of-flight spectroscopy (MALDI-TOF). Figure 4 displays the GPC and MALDI-TOF data for the block copolymer **1c**. The distribution of molecular weights is clearly a result of the anionic styrene polymerization and the MALDI-TOF spectra show that even a polymer with a polydispersity(PD) < 1.05 contains a variety of different molecular species with molecular weights ranging from 5500 up to 8000 $g\,mol^{-1}$ in this case.

Solid-state organization: Despite the superstructure formation of **1c** in cyclohexane, we were not able to observe the formation of any superstructure by thermal treatment of this material (i.e. slow or fast cooling from the melt). However, if solid samples of **1c** were prepared by slow evaporation of a cyclohexane solution (i.e. under equilibrium conditions), superstructure formation could be observed on different length scales. Figure 5 a shows the optical micrograph of a thin film of **1c** taken in differential interference contrast (DIC) indicating the formation of a ribbon-like structure. Transmission electron microscopy (TEM) studies could not extend our knowledge significantly. They showed that these extended moieties are composed of bundles of ribbons slightly tilted round the predominant direction (Figure 5 b). In particular, an aggregation of supramolecular cylinders such that isolated

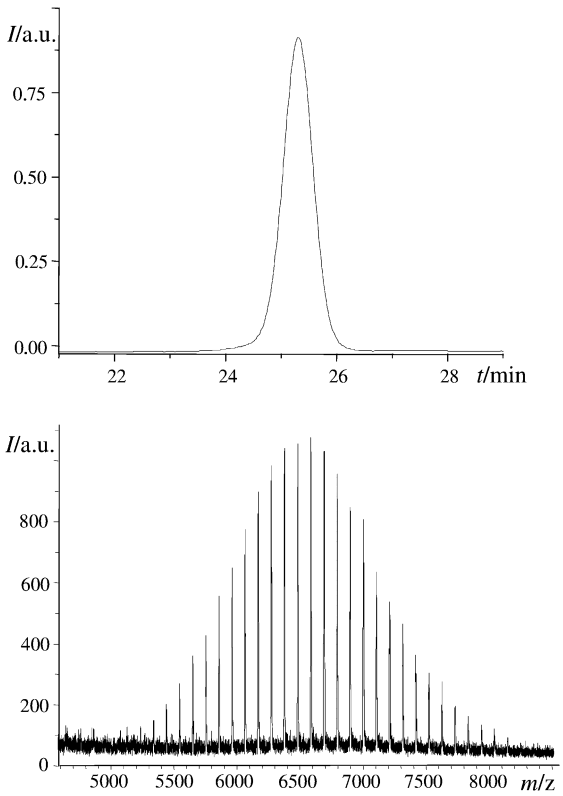

Figure 4. GPC and MALDI-TOF data of **1c**.

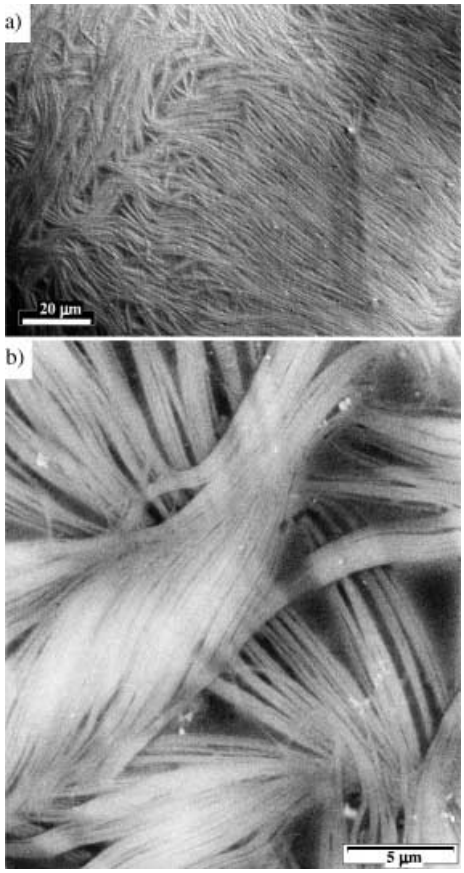

Figure 5. a) Optical micrograph of ribbon-like structures of **1c** imaged by differential interference contrast in reflected light. b) Electron micrograph of a similar sample (image taken at an electron energy loss of 235 eV for enhanced contrast).

channels are formed within a PS matrix (Figure 3a, model 1) could not be demonstrated by the TEM images.

Therefore, scattering experiments were conducted on samples of **1c** prepared under the same conditions (slow solvent evaporation) to investigate the solid-state structure of the material.

X-ray scattering of films (slow solvent evaporation) of **1c** performed in a powder diffractometer on a glass substrate show very strong first- ($n=1$) and second-order ($n=2$) reflections (Figure 6). Higher order reflections ($n=4$, 6, 10)

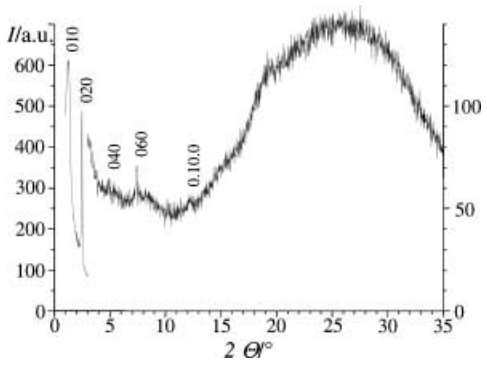

Figure 6. X-ray scattering of films of **1c** (the intensity scale of the scattering curve beyond 3° (right) is magnified by a factor of 5).

are present with much lower intensity as well as a diffuse reflection originating from both the amorphous PS matrix and the glass substrate. Because the scattering curve is recorded in reflection the occurring reflections can be assigned to a periodic lattice of layers oriented parallel to the substrate. The layer distance determined from these reflections is $d=71.6$ Å.

Reflections for additional directions of beam incidence were explored by complementary electron diffraction studies. However, the proper preparation of the samples used for electron diffraction turned out to be an essential task. During the investigations it became evident that solvent was retained in the samples and evaporated in the high vacuum of the transmission electron microscope (TEM), a fact confirmed by NMR spectroscopy (see below). The evaporating solvent left a volume deficiency in the sample destroying any order in the solid. Reproducible results were obtained only when the samples were inserted into the high vacuum of the electron microscope in a cryo-transfer holder at temperatures below 0 °C. The electron microscopic investigation was then carried out at temperatures below −50 °C to avoid the escape of the trapped solvent. With this technique a number of similar electron diffraction patterns of samples cast from cyclohexane could be obtained. As a common feature, an oriented set of point reflections was observed, resembling on first sight fiber diagrams consisting of an equator and a first layer line, superimposed by a diffuse isotropic halo that originates from the amorphous polystyrene. A typical diffraction pattern is shown in Figure 7. In some cases additional reflections are observed on a second layer line (Table 1).[18]

The meridian in the fiber-like diffraction patterns coincides in all cases with the axial direction of oriented strands recognizable in the corresponding electron micrographs.

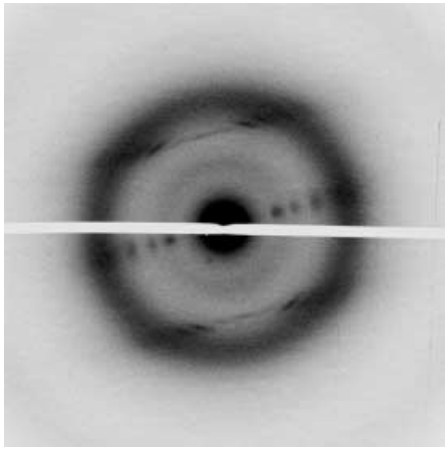

Figure 7. Electron diffraction pattern at perpendicular beam incidence.

Table 1. Observed and calculated reflections from X-ray data at room temperature, electron diffraction data at T < −50 °C.

h k l	d_{obs} [Å]	d_{calcd} [Å]	*h k l*	d_{obs}[b] [Å]	d_{calcd} [Å]
X-ray, powder diffraction			electron diffraction, 1st layer line		
0 1 0	71.0	71.60	0 0 1	6.22	6.20
0 2 0	35.7	35.80	2 0 1	5.99	5.99
0 4 0	17.8	17.90	4 0 1	5.51	5.46
0 6 0	11.9	11.93	5 0 1	5.15	5.15
0.10.0	7.2	7.16	0 1 1	6.18	6.18
electron diffraction, equator			2 1 1	5.94	5.97
			4 1 1	5.46	5.45
2 0 0		23.1	5 1 1	5.10	5.13
2 1 0	present[a]	22.0	5 2 1	5.09	5.09
2 2 0		19.4	0 3 1	6.00	6.00
4 0 0		11.6	3 3 1	5.58	5.59
4 1 0	present[a]	11.4	6 3 1	4.72	4.73
4 2 0		11.0	7 3 1	4.45	4.44
6 0 0		7.71	8 3 1	4.18	4.16
6 1 0	present[a]	7.66	4 4 1	5.23	5.22
6 2 0		7.53	6 4 1	4.64	4.66
8 0 0		5.78	electron diffraction, 2nd layer line		
8 1 0	present[a]	5.76	0 2 2	3.08	3.09
8 2 0		5.71	0 3 2	3.07	3.07
			0 5 2	3.03	3.03

[a] *d* spacings from reflections on the equator cannot be evaluated with sufficient precision owing to superposition. [b] Average value of the data taken from various diffraction patterns.

Although the reflections on the equator are less affected from the superimposition by the amorphous halo their positions cannot be measured with sufficient precision. The corresponding data were therefore neglected for the data refinement. Reflections on the layer lines are more distinct and turned out to be appropriate for data evaluation.

For indexing the electron diffraction patterns it is assumed that the reciprocal lattice vector a^* is oriented along the equator (ignoring an eventual superposition of several adjacent reflections) and c^* (equivalent to the repeat unit along the oriented strands) along the meridian. In this system of coordinates the X-ray reflections (Figure 6) have to be indexed as $0k0$. The predominant electron diffraction pattern (Figure 7) therefore contains the $h0l$ reflections. The sequence of the reflections along a layer line point to a value in the region of 45 Å for the *a* parameter. With this value in mind the

innermost equatorial reflection is the 200 reflection. The position of the maximum of intensity may vary by superimposition of adjacent reflections.[19] Close inspection of the electron diffraction patterns, in particular of the sequence of reflections along the "layer lines", shows that the diffraction patterns differ from fiber diagrams. They are diffraction patterns of single crystals with superimpositions of a varying number of reflections of adjacent zones.

The position of the first layer line varies between 5.9 and 6.2 Å corresponding to the prevailing index k for the meridional reflection. The d spacings from the X-ray diffractogram and from the reflections on the first and second layer in the electron diffraction patterns were used in a least-squares analysis to refine the lattice parameters (Table 1). The observed reflections are compatible with an orthorhombic cell with the lattice constants

$a = 46.1$, $b = 71.6$, $c = 6.2$ Å, $Z = 2$ ($V = 20465$ Å^3).

The d values calculated for the equatorial reflections show that the observed maxima of intensity are superpositions of at least three adjacent reflections with varying index k (and unknown intensity ratio). With the assumption that the block copolymer has an average molecular weight of 6500 Dalton and that three molecules of cyclohexane are attributed to one macrocycle, a density of 1.10 g cm^{-3} can be calculated for two molecules present in the unit cell. The presence of cyclohexane in the solid state structure is supported by the observation that films of the block copolymer cast from cyclohexane and stored for seven days at ambient conditions contain between two and four molecules of cyclohexane per coil – ring – coil block copolymer molecule, as determined by proton NMR analysis. In addition, the single-crystal X-ray analysis of several similar macrocycles show that the compounds crystallize as solvates to fill the empty interior of the rings.[7g,20]

In all electron diffraction patterns high intensity is observed near reflections $3k1$, $4k1$, and $5k1$ and the corresponding reflections with the Miller index $\bar{h}$ instead of h. This observation suggests that the macrocycles form a herringbone-like packing in the crystalline layers of the material. These crystalline layers are separated by amorphous layers that contain the polystyrene substituents. The thickness of one double layer consisting of one crystalline layer (rings) and one amorphous layer (PS) is 72 Å. A model for the state of order in the investigated samples is shown in Figure 8. It shows that the coil – ring – coil block copolymer **1c** in the solid state forms a *lamellar morphology* and that in solution the initially formed supramolecular cylindrical brushes *do not form isolated channels* within the amorphous PS matrix. The ability of the block copolymers to form a lamellar superstructure is a result of the attachment of the PS side chains at only two positions of the ring.

As shown previously, the rings in adjacent stacks are tilted with respect to each other so that herringbone packing is the result. This tilt is remarkable with respect to the solid-state structures of rod – coil block copolymers. In a solvent, preferential to the coil block, the aggregation block copolymer can lead to a tilt of the rod blocks with respect to the interface separating the rod and the coil blocks.[21] This gives the coil blocks a larger area per junction to the rod blocks and leads to reduced chain stretching of the coil blocks. At the same time the interface between the rod and the coil block is increased by the tilt so that the experimentally observed tilt angle is a minimum of the energetic penalties associated with chain stretching and interface separating (Figure 9a).[22]

In case of the coil – ring – coil block copolymers described here, the tilt of the macrocycles with respect to the stack axis does not give the coil blocks a larger area per junction to the ring blocks. The increased separation of the junctions along the stacking axis (c axis) is accompanied by a decreased separation of the junction points along the a axis (Figure 9b). Therefore, the tilt is dominated by the crystallization of the rigid parts of the block copolymer that try to minimize the contact with the cyclohexane.[23]

The observation that upon evaporation of the cyclohexane the periodicity of the columnar stacking is lost further supports the assumption that the included cyclohexane molecules are located in the crystalline layers. Again, this is closely analogous to the crystal structures of various macrocycles. Moreover, the fact that the superstructure is formed only in the presence of an appropriate solvent indicates that it plays a crucial role not only for the aggregation of these materials and the transition from the solution to the solid state but also for the stabilization of the rigid parts of the block copolymer in the crystalline state.

Conclusion

We have shown that the coil – ring – coil block copolymer **1c** aggregates by slow solvent evaporation under equilibrium conditions into a (solvated) material with a lamellar morphology. The rigid cyclic domains crystallize and are separated by amorphous PS layers. Driving forces are the microphase separation of the rigid and the coil blocks and the solvophobic aggregation of the macrocyclic segments into crystalline domains. This morphology is different from the aggregate structure in solution where individual stacks are covered by the PS shell. These results show that a

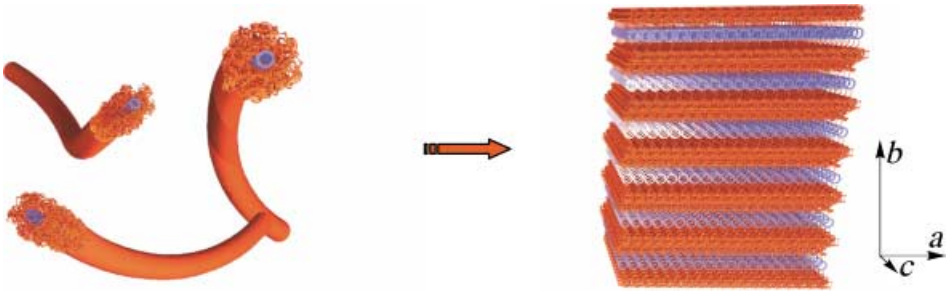

Figure 8. Aggregation of supramolecular polymer brushes in the solid state into a lamellar superstructure.

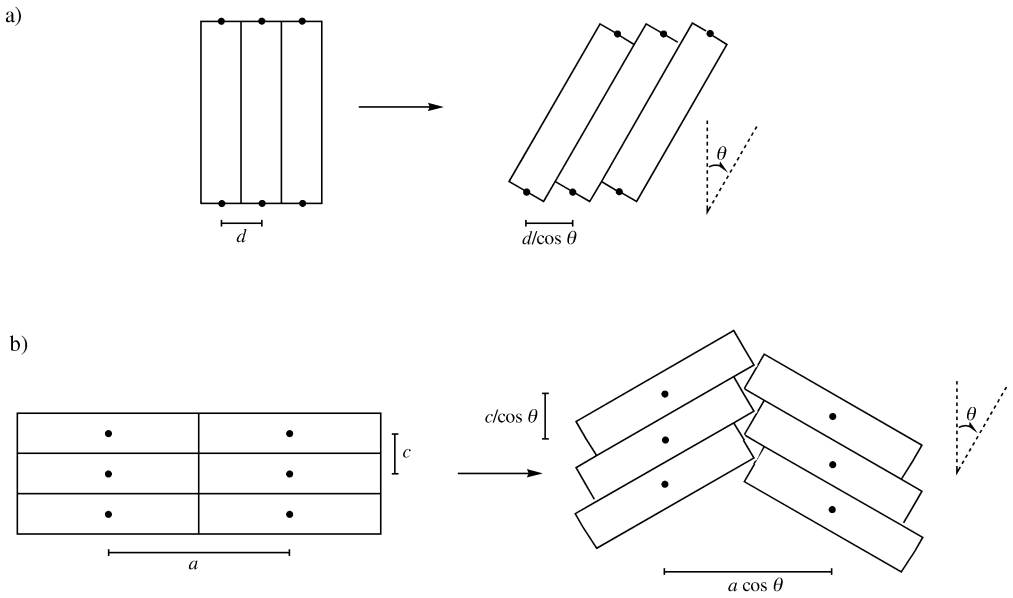

Figure 9. a) In rod–coil block copolymers the rod tilt increases the average separation between junctions (here "●") (adapted from ref. [21]). b) In **1c** the ring tilt increases the distance between junctions within a stack (*c* axis) but the distance between junctions of adjacent stacks (*a* axis) is reduced.

prediction of the solid state structure on the basis of the solution structure and vice versa is not possible.

Ongoing investigations on coil–ring–coil block copolymers with different numbers and kinds of coil segments will show how these factors influence the superstructure of the materials. Of special interest is the synthesis and investigation of intraannular functionalized ring-coil block copolymers and their aggregation to intraannular functionalized nanorods.

Experimental Section

General methods: Commercially available chemicals were used as received. THF was distilled over potassium prior to use. Piperidine and pyridine were distilled from CaH_2 and stored under argon. Dichloromethane of quality "water-free" was purchased and used as received. 4-(Dimethylamino)-pyridinium/*p*-toluenesulfonate (DMAP/*p*-TsOH) was prepared by mixing equimolar amounts of the acid and the base in dichloromethane and precipitation of the salt by the addition of diethyl ether. After filtration and drying in vacuum the catalyst was used without further purification. All other solvents (p.a. quality) and reagents were used as received. Unless otherwise stated, acid, base, and salt solutions are aqueous. ^{1}H NMR and ^{13}C NMR spectra were recorded on a Bruker AC-300 (300 MHz for proton, 75.48 MHz for carbon). Thin-layer chromatography was performed on aluminum plates pre-coated with Merck 5735 silica gel 60 F_{254}. Column chromatography was performed with Merck silica gel 60 (230–400 mesh). Radial chromatography was performed with Merck silica gel 60 PF_{254} containing $CaSO_4$. The gel permeation chromatograms were measured in THF (flow rate 1 mL min^{-1}) at room temperature, using a combination of three styragel columns (porosity 10^3, 10^5, and 10^6), an RI detector and an UV detector operating at $\lambda = 254$ nm. The molecular weight was obtained from polystyrene-calibrated SEC columns. The matrix-assisted laser desorption ionization time-of-flight measurements were carried out on a Bruker reflex spectrometer (Bruker, Bremen), incorporating a 337 nm nitrogen laser with a 3 ns pulse duration (10^6–10^7 W cm^{-1}, 100 μm spot diameter). The instrument was operated in a linear mode with an accelerating potential of 33.65 kV. The mass scale was calibrated with polystyrene ($M_p = 4700$), using a number of resolved oligomers. Samples were prepared by dissolving the macrocycle in THF at a concentration of 10^{-4} mol L^{-1}. A 10 μL portion of this solution and 10 μL of a 10^{-3} mol L^{-1} silver trifluoroacetate (lithium trifluoroacetate, respectively) solution were added to 10 μL of a 0.1 mol L^{-1} matrix solution, dissolved in THF. In all cases 1,8,9-trihydroxyanthracene (Aldrich, Steinheim) was used as matrix. A 1 μL portion of this mixture was applied to the multistage target and airdried.[24] Microanalysis was performed at the University of Mainz. Melting points were measured with a Reichert hot stage apparatus and are uncorrected.

Anionic polymerization: The anionic polymerizations were carried out in cyclohexane under a nitrogen atmosphere in a glass ampoule. Cyclohexane was purified by titration of diphenylethene using *n*BuLi until the color of the solution turned red and was distilled under reduced pressure. Styrene was purified by stirring with solid fluorenyllithium (from fluorene and *n*BuLi and removal of the solvent) for several minutes at room temperature and distilled under reduced pressure. *sec*-Butyllithium (1.3 M solution in cyclohexane/hexane 92/2 v/v) and CO_2 were used as received.

X-ray scattering: X-ray scattering was performed on a Philips PW 1820 X-ray diffractometer in reflection mode ($Cu_{K\alpha}$, 1.541 Å). Samples were prepared by drop casting a solution of **1c** in cyclohexane on a glass slide and slow evaporation of the solvent in the presence of additional cyclohexane (in a slightly covered desiccator).

Electron diffraction: Electron diffraction was performed on a LEO 912 transmission electron microscope operated at high voltage (120 kV). The instrument was equipped with an integrated electron energyloss spectrometer. The width of the energy window was set to $\delta E = 15$ eV. The camera length was calibrated by using a TlCl powder sample. Once it was evident that solvent was retained in the samples which could escape in the high vacuum of the TEM, the samples were cast onto carbon-coated glass slides. Sample preparation was performed as described above. The carbon films with the sample were floated off the glass and transferred onto copper specimen grids. They were inserted into the high vacuum of the electron microscope in a GATAN cryo-transfer holder, Model 626, at temperatures below 0 °C. The electron microscopic investigation was then carried out at temperatures below −50 °C.

1-*tert*-Butyl-3-[2-{4-(2-triethylsilylethynyl)phenyl}ethynyl]-5-(2-triisopropylsilylethynyl)benzene (3): 4-Bromoiodobenzene (10.0 g, 35.3 mmol) and triphenylposphine (0.38 g) were dissolved in piperidine (245 mL) under argon. The solution was cooled to 0 °C and 2-triethylsilylacetylene (5.44 g, 38.7 mmol), $[PdCl_2(PPh_3)_2]$ (0.38 g) and CuI (0.19 g) were added. The mixture was stirred overnight at room temperature. The solution was then heated to 50 °C for 1 h and 1-ethynyl-3-(2-triisopropylsilylethynyl)-5-*tert*-butylbenzene[11a] (14.13 g, 41.72 mmol) was added and the solution stirred at this temperature for four days. After the mixture was cooled to room temperature, diethyl ether and water were added, the organic phase was

separated, and washed with water, 10% acetic acid, 10% sodium hydroxide, and saturated NaCl solution. After the solution was dried over $MgSO_4$ and the solvent was evaporated, the crude product was purified by column chromatography using petroleum ether as eluent ($R_f = 0.38$) to give **3** (17.5 g, 91%) as a white powder. ^{1}H NMR ($CDCl_3$): $\delta = 0.66$ (q, $J =$ 7.99 Hz, 6H), 1.03 (t, $J = 7.62$ Hz, 9H), 1.13 (s, 21H), 1.31 (s, 9H), 7.40 – 7.50 ppm (m, 7H); ^{13}C NMR ($CDCl_3$): $\delta = 4.43$, 7.47, 11.36, 31.10, 34.68, 88.96, 90.64, 90.97, 93.87, 105.92, 106.72, 122.82, 123.11, 123.25, 123.54, 128.79, 129.04, 131.40, 131.98, 132.39, 151.53 ppm; MS(FD): m/z: 552.7 [M^+], 1105.1 [$2M^+$]; elemental analysis calcd (%) for $C_{37}H_{52}Si_2$ (552.98): C 80.36, H 9.48; found: C 80.31, H 9.59.

1-*tert*-Butyl-3-[2-(4-ethynylphenyl)ethynyl]-5-(2-triisopropylsilylethynyl)-benzene (4): K_2CO_3 (18.6 g, 134 mmol) was added to a solution of **3** (17.55 g, 32 mmol) in THF/methanol (2:1) (250 mL) and stirred for four days at room temperature. Diethyl ether and water were added, the organic phase was separated and washed with water and saturated NaCl solution. After the solution was dried over $MgSO_4$ and the solvent was evaporated, the crude product was purified by recrystallization from a mixture of methanol/ethanol (3:1) to give **4** as a white powder (11.8 g, 83%). M.p.: 75 °C; ^{1}H NMR ($CDCl_3$): $\delta = 1.13$ (s, 21H), 1.31 (s, 9H), 3.16 (s, 1H), 7.40 – 7.50 ppm (m, 7H); ^{13}C NMR ($CDCl_3$): $\delta = 11.36$, 18.69, 31.10, 34.69, 78.92, 88.71, 90.70, 91.12, 106.69, 121.99, 122.74, 123.56, 128.79, 129.12, 131.50, 132.08, 132.39, 151.56 ppm; MS (FD): m/z: 438.2 [M^+], 879.3 [$2M^+$], 1318.3 [$3M^+$]; elemental analysis calcd (%) for $C_{31}H_{38}Si$ (438.72): C 84.87, H 8.73; found: C 84.88, H 8.69.

6-(3,5-Diiodophenoxy)hexyl benzoate (5): 3,5-Diiodophenol (5.28 g, 15.0 mmol), 6-bromo-1-hexanol (2.78 g, 15.0 mmol), and K_2CO_3 (4.26 g, 30.0 mmol) were stirred in DMF (30 mL) at 60 °C overnight under argon. After the mixture was cooled to room temperature, diethyl ether and water were added to the brown suspension and the organic phase was separated and washed four times with water, and then saturated NaCl solution and dried over $MgSO_4$. After filtration of the solution and evaporation of the solvent, the crude product was purified by column chromatography using diethyl ether/petroleum ether (3:1) as eluent ($R_f = 0.48$). After evaporation of the solvent and drying under vacuum, 6-(3,5-diiodophenoxy)-hexan-1-ol was obtained as a white powder (6.5 g, 79%). M.p.: 46 °C; ^{1}H NMR ($CDCl_3$): $\delta = 1.34 – 1.47$ (m, 4H), 1.57 (m, 2H), 1.74 (m, 2H), 3.63 (t, $J =$ 6.65 Hz, 2H), 3.86 (t, $J = 6.65$ Hz, 2H), 7.17 (d, $J = 1.27$ Hz, 2H), 7.58 ppm (t, $J = 1.27$ Hz, 1H); ^{13}C NMR ($CDCl_3$): $\delta = 25.42$, 25.72, 28.95, 32.57, 62.79, 68.29, 94.54, 123.40, 137.30, 159.84 ppm; MS (FD): m/z: 445.6 [M^+]; elemental analysis calcd (%) for $C_{12}H_{16}I_2O_2$ (446.06): C 32.31, H 3.62; found: C 33.11, H 3.73.

6-(3,5-Diiodophenoxy)hexan-1-ol (6.49 g, 14.5 mmol) and benzoyl chloride (2.1 g, 14.9 mmol) were dissolved in THF (20 mL) under argon. The mixture was cooled to 0 °C and pyridine (1.5 g, 18.9 mmol) was slowly added (accompanied with the formation of a white precipitate). After the mixture was stirred overnight at room temperature, diethyl ether and water were added and the organic phase was separated and washed with water, 10% acetic acid, 10% sodium hydroxide, and saturated NaCl solution. The organic phase was dried over $MgSO_4$ and after filtration and evaporation of the solvent, the crude product was purified by column chromatography using a mixture of dichloromethane/petroleum ether (1:1) as eluent ($R_f =$ 0.36). After evaporation of the solvent and drying under vacuum, **5** was obtained as a white powder (7.0 g, 88%). M.p.: 56 °C; ^{1}H NMR ($CDCl_3$): $\delta = 1.45 – 1.55$ (m, 4H), 1.70 – 1.85 (m, 4H), 3.87 (t, $J = 6.32$ Hz, 2H), 4.32 (t, $J = 6.32$ Hz, 2H), 7.16 (d, $J = 1.25$ Hz, 2H), 7.35 – 7.45 (m, 2H), 7.50 – 7.60 (m, 2H), 7.95 – 8.05 ppm (m, 2H); ^{13}C NMR ($CDCl_3$): $\delta = 25.63$, 25.75, 28.60, 28.88, 64.82, 68.20, 94.56, 123.35, 128.31, 129.48, 130.38, 132.81, 137.29, 159.79, 166.59 ppm; MS (FD): m/z: 549.6 [M^+]; elemental analysis calcd (%) for $C_{19}H_{20}I_2O_3$ (549.8): C 41.48, H 3.66; found: C 41.32, H 3.83.

6-[3,5-Bis{2-(4-{2-[3-*tert*-butyl-5-(2-triisopropylsilylethynyl)]phenylethynyl}phenylethynyl)}phenoxy]hexyl benzoate (6): [$Pd_2(dba)_3$] (85 mg; dba = dibenzylideneacetone) and CuI (43 mg) were added to a solution of **4** (2.9 g, 6.6 mmol), **5** (1.82 g, 3.3 mmol), and triphenylphosphine (85 mg) in triethylamine (20 mL) and the mixture was stirred at room temperature under argon for three days. Then, the solution was heated for an additional hour to 50 °C. After the mixture was cooled to room temperature, diethyl ether and water were added, and the organic phase was separated and washed with water, 10% acetic acid, 10% sodium hydroxide, and saturated NaCl solution. After the solution was dried over $MgSO_4$ and the solvent was evaporated, the crude product was purified by column chromatography using petroleum ether/dichloromethane (2:1) as eluent ($R_f = 0.53$). After evaporation of the solvent and drying under vacuum, **6** was obtained as an almost white powder (3.0 g, 78%). M.p.: 72 °C; ^{1}H NMR ($CDCl_3$): $\delta = 1.12$ (s, 42H), 1.32 (s, 18H), 1.50 – 1.60 (m, 4H), 1.75 – 1.90 (m, 4H), 3.99 (t, $J =$ 6.32 Hz, 2H), 4.34 (t, $J = 6.62$ Hz, 2H), 7.02 (d, $J = 1.27$ Hz, 2H), 7.29 (t, $J =$ 1.25 Hz, 1H), 7.38 – 7.55 (m, 17H), 8.03 ppm (m, 2H); ^{13}C NMR ($CDCl_3$): $\delta = 11.32$, 18.67, 25.75, 25.84, 28.68, 29.04, 31.08, 34.67, 64.90, 68.09, 88.91, 89.42, 90.42, 90.65, 91.10, 106.65, 117.90, 122.74, 122.82, 123.18, 123.50, 124.29, 128.33, 128.79, 129.08, 129.52, 129.98, 131.59, 132.38, 132.83, 151.52, 152.29 ppm; MS (FD): m/z: 1169.8 [M^+]; elemental analysis calcd (%) for $C_{81}H_{94}O_3Si_2$ (1171.78): C 83.02, H 8.09; found: C 82.81, H 8.13.

6-[3,5-Bis(2-{4-[2-(3-*tert*-butyl-5-ethynyl)phenylethynyl]phenylethynyl})-phenoxy]hexyl benzoate (7): A solution of Bu_4NF in THF (1M, 5.5 mL, 5.5 mmol) was added to a solution of **6** (3.0 g, 2.57 mmol) in THF (10 mL). After the mixture was stirred overnight at room temperature, diethyl ether and water were added. The organic phase was separated and washed with water and saturated NaCl solution, and then dried over $MgSO_4$. After evaporation of the solvent, the crude product was purified by column chromatography using petroleum ether/dichloromethane (1:1) as eluent ($R_f = 0.55$). After evaporation of the solvent and drying under vacuum, **7** was obtained as a white powder (2.03 g, 93%). M.p.: 52 °C; ^{1}H NMR ($CDCl_3$): $\delta = 1.31$ (s, 18H), 1.50 – 1.60 (m, 4H), 1.75 – 1.90 (m, 4H), 3.06 (s.2H), 3.99 (t, $J = 6.15$ Hz, 2H), 4.33 (t, $J = 6.47$ Hz, 2H), 7.02 (d, $J =$ 1.42 Hz, 2H), 7.29 (t, $J = 1.42$ Hz, 1H), 7.35 – 7.55 (m, 17H), 8.00 – 8.05 ppm (m, 2H); ^{13}C NMR ($CDCl_3$): $\delta = 25.76$, 25.84, 28.68, 29.04, 31.05, 34.69, 64.90, 68.09, 77.18, 89.07, 89.41, 90.47, 90.89, 117.92, 122.09, 122.91, 123.10, 124.29, 128.33, 129.26, 129.45, 131.60, 132.25, 132.83, 151.52, 158.79 ppm; MS (FD): m/z: 858.0 [M^+]; elemental analysis calcd (%) for $C_{63}H_{54}O_3$ (859.10): C 88.08, H 6.34; found: C 88.06, H 6.28.

Macrocycle 8: A solution of **7** (0.60 g, 0.64 mmol) in pyridine (15 mL) was added to a suspension of CuCl (3.82 g) and $CuCl_2$ (0.75 g) in pyridine (120 mL) over 96 h at 55 °C. After completion of the addition, CH_2Cl_2 and water were added and the organic phase was separated and washed with water, 25% aqueous NH_3 solution (until the aqueous phase remained nearly colorless), 10% acetic acid, 10% sodium hydroxide, and saturated NaCl solution, and dried over $MgSO_4$. After evaporation of the solvent to about 20 mL, the coupling products were precipitated by the addition of methanol (100 mL) and collected by filtration. The crude product was purified by double column chromatography. The first used a mixture of petroleum ether/dichloromethane (1:3) as eluent ($R_f = 0.83$), the second used a mixture of petroleum ether/dichloromethane (1:2) as eluent ($R_f =$ 0.69). After evaporation of the solvent and drying under vacuum, pure **8** was obtained as a white powder (0.30 g, 50%). M.p.: > 250 °C (decomp); ^{1}H NMR ($CDCl_3$): $\delta = 1.32$ (s, 36H), 1.50 – 1.60 (m, 8H), 1.75 – 1.90 (m, 8H), 3.99 (t, $J = 6.15$ Hz, 4H), 4.33 (t, $J = 6.47$ Hz, 4H), 7.01 (d, $J = 1.40$ Hz, 4H), 7.33 (t, $J = 1.25$ Hz, 2H), 7.33 – 7.58 (m, 34H), 8.00 – 8.08 ppm (m, 4H); ^{13}C NMR ($CDCl_3$): $\delta = 25.78$, 25.86, 28.71, 29.07, 31.07, 34.80, 64.92, 68.09, 73.93, 81.32, 89.39, 89.46, 90.53, 90.75, 117.71, 121.84, 123.07, 123.25, 124.34, 128.35, 129.55, 131.65, 132.83, 133.13, 151.92, 158.89 ppm; GPC: single peak at $M_w = 2700$; MS (FD): m/z: 1713.9 [M^+]; elemental analysis calcd (%) for $C_{126}H_{104}O_6$ (1714.17): C 88.28, H 6.12; found: C 88.29, H 6.19.

Macrocycle 9: 10% potassium hydroxide (3 mL) was added to a solution of **8** (0.4 g, 0.23 mmol) in THF (20 mL). The mixture was refluxed at 66 °C overnight. The solvent volume was reduced to about 5 mL and the macrocycle was precipitated by the addition of methanol. After filtration and drying under vacuum, **9** was obtained as a white powder (0.3 g, 87%). M.p.: > 250 °C (decomp); ^{1}H NMR ($CDCl_3$): $\delta = 1.32$ (s, 36H), 1.35 – 1.68 (m, 12H), 1.75 – 1.88 (m, 4H), 3.66 (t, $J = 6.3$ Hz, 4H), 3.98 (t, $J = 6.57$ Hz, 4H), 7.01 (d, $J = 1.35$ Hz, 4H), 7.33 (t, $J = 1.25$ Hz, 2H), 7.51 (s, 20H), 7.52 – 7.55 ppm (m, 8H); ^{13}C NMR ($CDCl_3$): $\delta = 25.57$, 25.90, 29.20, 31.10, 32.76, 34.82, 62.92, 68.37, 74.03, 81.40, 89.46, 89.51, 90.59, 90.81, 117.85, 121.97, 123.14, 123.39, 124.45, 127.97, 129.45, 131.68, 133.19, 152.01, 159.03 ppm; GPC: single peak at $M_w = 2200$; MS (FD): m/z: 1504.4 [M^+]; elemental analysis calcd (%) for $C_{112}H_{96}O_4$ (1506.08): C 89.33, H 6.43; found: C 88.78; H 6.37.

PS-COOH (10): Cyclohexane (100 mL) and styrene (10 mL) were placed in an ampoule and the appropriate amount of *sec*-butyllithium was added through a syringe. After 3 h at room temperature, a small amount (~1 mL) of the solution was quenched with methanol (10 mL) and the molecular weight (peak molecular weight M_p is given here) and the polydispersity D of the polystyrene was determined by GPC analysis. The rest of the solution

was transferred into THF (500 mL) saturated with CO_2 and the resulting solution was acidified with methanolic HCl. After evaporation of the solvent the PS-carboxylic acid was purified by column chromatography using toluene as eluent to remove all impurities ($R_f \sim 0.9$). The free acid was obtained by elution with THF and evaporation of the solvent (isolated yields: 60–80%). ^{1}H NMR ($CDCl_3$): $\delta = 0.6-0.8$ (br, $CH_3CH_2CH(PS)CH_3$, 6H), 0.8–2.6 (br), 3.3–3.5 (br, (PS)PhC*H*-COOH, 1H), 6.3–7.5 ppm (br). From the MALDI-TOF data of the acid the degree of polymerization (n) for the most intensive peak can be calculated.

10a: GPC (methanol-quenched anion): $M_w = 1030\ g\,mol^{-1}$; $D = 1.19$; MS(MALDI-TOF) (PS-COOH, most intensive peak): m/z: 1145.2 $[M+Ag^+]$ ($n = 9$); elemental analysis calcd (%) for $C_{77}H_{82}O_2$ (1039.59): C 88.96, H 7.97; found: C 88.05, H 8.14.

10b: GPC (methanol-quenched anion): $M_w = 1580\ g\,mol^{-1}$; $D = 1.16$; MS(MALDI-TOF) (PS-COOH, most intensive peak): m/z: 1665.4 $[M+Ag^+]$ ($n = 14$); elemental analysis calcd (%) for $C_{117}H_{122}O_2$ (1560.39): C 90.05, H 7.90; found: C 88.89, H, 8.22.

10c: GPC (methanol-quenched anion): $M_w = 2430\ g\,mol^{-1}$; $D = 1.06$; MS(MALDI-TOF) (PS-COOH, most intensive peak): m/z: 2607.5 $[M+Ag^+]$ ($n = 23$); elemental analysis calcd (%) for $C_{189}H_{194}O_2$ (2497.83): C 90.88, H 7.84, found: C 90.34, H 7.72.

10d: GPC (methanol-quenched anion): $M_w = 3650\ g\,mol^{-1}$; $D = 1.10$; MS(MALDI-TOF) (PS-COOH, most intensive peak): $m/z = 3543.6$ $[M+Ag^+]$ ($n = 32$); elemental analysis calcd (%) for $C_{261}H_{266}O_2$ (3435.27): C 91.25, H 7.82; found: C 91.30, H 7.45.

10e: GPC (methanol-quenched anion): $M_w = 5600\ g\,mol^{-1}$; $D = 1.03$; MS(MALDI-TOF) (PS-COOH, most intensive peak): m/z: 5319.5 $[M+Li^+]$ ($n = 50$); elemental analysis calcd (%) for $C_{405}H_{410}O_2$ (5310.15): C 91.60, H 7.80, found: C 91.24, H 7.94.

Block copolymers 1: Compounds **9** (50 mg, 0.0332 mmol), **10** (0.0731 mmol), and DMAP/*p*-TsOH (43 mg, 0.15 mmol) were dissolved in dry CH_2Cl_2 (15 mL) by gentle warming. After the mixture was cooled to room temperature, diisopropyl carbodiimide (18 mg, 0.15 mmol) was added and the mixture stirred for three days. The solvent was evaporated and the crude product was purified by column chromatography using dichloromethane as eluent ($R_f = 0.93$). After evaporation of the solvent and drying under vacuum, **1** was obtained as a white powder. ^{1}H NMR ($CDCl_3$): $\delta = 0.6-0.8$ (br, $CH_3CH_2CH(PS)CH_3$, 6H), 0.8–2.6 (br), 1.32 (s, 36H) 3.0–3.2 (br, (PS)PhC*H*-COOH, 1H), 3.7–4.0 (br, Ar-O-CH_2-; CH_2-OCO(PS)) 6.3–7.4 (br), 7.33 (m, 2H), 7.51 (s, 20H), 7.54 ppm (m, 8H). From the MALDI-TOF data the degree of polymerization ($n+n$) of the styrene for the most intensive peak can be calculated.

1a: (32% yield) GPC: $M_w = 4710\ g\,mol^{-1}$; $D = 1.05$; MS(MALDI-TOF) (most intensive peak): m/z: 3464 $[M+Na^+]$ ($n+n = 17$); elemental analysis calcd (%) for $C_{258}H_{248}O_6$ (3445.07): C 90.00, H 7.27; found: C 88.05, H 7.98.

1b: (86% yield) GPC: $M_w = 5460\ g\,mol^{-1}$; $D = 1.09$; MS(MALDI-TOF) (most intensive peak): m/z: 4194 $[M+Na^+]$ ($n+n = 27$); elemental analysis calcd (%) for $C_{322}H_{312}O_6$ (4278.34): C 90.43, H 7.37; found: C 87.69, H 8.01.

1c: (84% yield) GPC: $M_w = 8320\ g\,mol^{-1}$; $D = 1.05$; MS(MALDI-TOF) (most intensive peak): m/z: 6587 $[M+Na^+]$ ($n+n = 47$); elemental analysis calcd (%) for $C_{498}H_{488}O_6$ (6569.86): C 91.04, H 7.50; found: C 90.74, H 7.72.

1d: (64% yield) GPC: $M_w = 10100\ g\,mol^{-1}$; $D = 1.04$; MS(MALDI-TOF) (most intensive peak): m/z: 8360 $[M+Na^+]$ ($n+n = 64$); elemental analysis calcd (%) for $C_{634}H_{624}O_6$ (8340,58): C 91.29, H 7.56; found: C 90.59, H 7.99.

1e: (39% yield) GPC: $M_w = 13470\ g\,mol^{-1}$; $D = 1.06$; MS(MALDI-TOF) (most intensive peak): m/z: 11880 $[M+Ag^+]$ ($n+n = 97$); elemental analysis calcd (%) for $C_{898}H_{888}O_6$ (11777.86): C 91.57 H 7.62; found: C 91.32, H 7.88.

[1] For some recent examples of complex superstructures formed by rod–coil block copolymers see, for example: a) E. R. Zubarev, M. U. Pralle, L. Li, S. I. Stupp, *Science* **1999**, *283*, 523–526; b) J. T. Chen, E. L. Thomas, C. K. Ober, G.-P. Mao, *Science* **1996**, *273*, 343–346; c) S. A. Jenekhe, X. L. Chen, *Science* **1999**, *283*, 372–375; d) H.-A. Klok, J. F. Langenwalter, S. Lecommandoux, *Macromolecules* **2000**, *33*, 7819–7826; e) H. Engelkamp, S. Middelbeek, R. J. M. Nolte, *Science* **1999**, *284*, 785–788; f) M. Lee, Y.-S. Jeong, B.-K. Cho, N.-K. Oh, W.-C. Zin, *Chem. Eur. J.* **2002**, *8*, 876–883; g) J. Raez, I. Manners, M. A. Winnik, *J. Am. Chem. Soc.* **2002**, *124*, 10381—10395.

[2] Reviews about rod–coil block copolymers: a) M. Lee, B.-K. Cho, W.-C. Zin, *Chem. Rev.* **2001**, *101*, 3869–3892; b) H.-A. Klok, S. Lecommandoux, *Adv. Mater*. **2001**, *13*, 1217–1229; c) G. Mao, C. K. Ober, *Acta Polymer*. **1997**, *48*, 405–422.

[3] a) S. Rosselli, A.-D. Ramminger, T. Wagner, B. Silier, S. Wiegand, W. Häußler, G. Lieser, V. Scheumann, S. Höger, *Angew. Chem.* **2001**, *113*, 3234–3237; *Angew. Chem. Int. Ed*. **2001**, *40*, 3138–3141; b) S. Höger, K. Bonrad, S. Rosselli, A.-D. Ramminger, T. Wagner, B. Silier, S. Wiegand, W. Häußler, G. Lieser, V. Scheumann, *Macromol. Symp.* **2002**, *177*, 185–191.

[4] Reviews about shape-persistent macrocycles: a) J. S. Moore, *Acc. Chem. Res.* **1997**, *30*, 402–413; b) S. Höger, *J. Polym. Sci, Part A* **1999**, *37*, 2685–2698; c) M. M. Haley, J. J. Pak, S. C. Brand, *Topic Curr. Chem.* **1999**, *201*, 81–130; d) C. Grave, A. D. Schlüter, *Eur. J. Org. Chem.* **2002**, 3075–3098.

[5] For the concept of intraannular functional groups, see, for example: a) F. Vögtle, P. Neumann, *Tetrahedron* **1970**, *26*, 5299–5318; b) E. Weber, F. Vögtle, *Chem. Ber.* **1976**, *109*, 1803–1831.

[6] For shape-persistent macrocycles containing intraannular functional groups, see, for example: a) H. L. Anderson, J. K. M. Sanders, *J. Chem. Soc. Chem. Commun.* **1992**, 946–947; b) S. Anderson, U. Neidlein, V. Gramlich, F. Diederich, *Angew. Chem.* **1995**, *107*, 1722–1726; *Angew. Chem. Int. Ed. Engl.* **1995**, *34*, 1596–1600; c) D. L. Morrison, S. Höger, *J. Chem. Soc. Chem. Commun.* **1996**, 2313–2314; d) Y. Tobe, N. Utsumi, K. Kawabata, A. Nagano, K. Naemura, *Angew. Chem.* **1998**, *110*, 1347–1349; *Angew. Chem. Int. Ed. Engl.* **1998**, *37*, 1285–1287; e) S. Höger, A.-D. Meckenstock, *Chem. Eur. J.* **1999**, *5*, 1686–1691; f) U. Lehman, A. D. Schlüter, *Eur. J. Org. Chem.* **2000**, 3483–3487; g) Y. Hosokawa, T. Kawase, M. Oda, *J. Chem. Soc. Chem. Commun.* **2001**, 1948–1949; h) M. Fischer, S. Höger, *Eur. J. Org. Chem.* **2003**, 441–446.

[7] For channel structures based on shape-persistent macrocycles see for example: a) D. Venkataraman, S. Lee, J. Zhang, J. S. Moore, *Nature* **1994**, *371*, 591–593; b) D. T. Bong, T. D. Clark, J. R. Granja, M. R. Ghadiri, *Angew. Chem.* **2001**, *113*, 1016–1041; *Angew. Chem. Int. Ed. Engl.* **2001**, *40*, 988–1011; c) G. Gattuso, S. Menzer, S. A. Nepogodiev, J. F. Stoddart, D. J. Wiliams, *Angew. Chem.* **1997**, *107*, 1615–1617; *Angew. Chem. Int. Ed. Engl.* **1997**, *36*, 1451–1454; d) O. Henze, D. Lentz, A. D. Schlüter, *Chem. Eur. J.* **2000**, *6*, 2362–2367; e) P. Müller, I. Usón, V. Hensel, A. D. Schlüter, G. M. Sheldrick, *Helv. Chim. Acta* **2001**, *84*, 778–785; f) R. A. Pascal, Jr., L. Barnett, X. Qiao, D. M. Ho, *J. Org. Chem*. **2000**, *65*, 7711–7717; g) S. Höger, D. L. Morrison, V. Enkelmann, *J. Am. Chem. Soc.* **2002**, *124*, 6734–6736.

[8] This is remarkable in the context that shape-persistent macrocycles of similar structure with oligo-alkyl side chains of defined length do not dissolve in this solvent. This shows the superior solubilizing properties of PS oligomers over oligo-alkyl substituents.

[9] The investigation of the exact nature of the driving force for the aggregation of the ring-coil block copolymers is currently under way.

[10] U. Lauter, W. H. Meyer, G. Wegner, *Maromolecules* **1997**, *30*, 2092–2102.

[11] For a template-directed approach towards these structures, see also: a) S. Höger, A.-D. Meckenstock, H. Pellen, *J. Org. Chem*. **1997**, *62*, 4556–4567; b) S. Höger, A.-D. Meckenstock, *Tetrahedron Lett*. **1998**, *39*, 1735–1736; c) S. Höger, *Macromol. Symp.* **1999**, *142*, 185–191.

[12] P. Siemsen, R. C. Livingston, F. Diederich, *Angew. Chem.* **2000**, *112*, 2740–2767; *Angew. Chem. Int. Ed.* **2000**, *39*, 2632–2657.

[13] P. Fitton, A. E. Rick, *J. Organomet. Chem.* **1971**, *28*, 287–291.

[14] a) C. Eaborn, D. R. M. Walton, *J. Organomet. Chem.* **1965**, *4*, 217–228; b) C. Rücker, *Chem. Rev.* **1995**, *95*, 1009–1064.

[15] S. Höger, K. Bonrad, L. Karcher, A.-D. Meckenstock, *J. Org. Chem*. **2000**, *65*, 1588–1889.

[16] a) J. C. M. van Hest, D. A. P. Delnoye, M. W. P. L. Baars, C. Ellisen-Román, M. H. P. van Genderen, E. W. Meijer, *Chem. Eur. J.* **1996**, *2*, 1616–1626; b) A. Hirao, H. Nagahama, T. Ishizone, S. Nakahama, *Macromolecules* **1993**, *26*, 2145–2150.

[17] J. S. Moore, S. I. Stupp, *Macromolecules* **1990**, *23*, 65–70.

[18] Occasionally the layer lines show continuous intensity with some sampling. We cannot exclude the fact that this feature is an indication of partially evaporated solvent.

[19] As mentioned before, the reflections on the equator are smeared out due to the overlap of reflection spikes owing to the necessarily small

sample thickness and the small distance between adjacent planes in b^* direction (i.e. the superposition of $h10$ and $h20$ with $h00$ reflections).
[20] S. Höger, V. Enkelmann, *Angew. Chem.* **1995**, *107*, 2717 – 2919; *Angew. Chem. Int. Ed. Engl.* **1995**, *34*, 2713 – 2716.
[21] a) A. Halperin, *Europhys. Lett.* **1989**, *10*, 549 – 553; b) T. Vilgis, A. Halperin, *Macromolecules* **1991**, *24*, 2090 – 2095.
[22] J. T. Chen, E. L. Thomas, C. K. Ober, S. S. Hwang, *Macromolecules* **1995**, *28*, 1688 – 1697.
[23] It can be assumed that the pore size of the columns decreases with increasing tilt angle of the macrocycles reducing the amount of cyclohexane occupying the empty space.
[24] S. Höger, J. Spickermann, D. L Morrison, P. Dziezok, H. J. Räder, *Macromolecules* **1997**, *30*, 3110 – 3111.

Received: January 31, 2003 [F4796]

